

Published in final edited form as:

Nat Struct Mol Biol. ; 18(12): 1331–1335. doi:10.1038/nsmb.2189.

Exploiting oncogene-induced replicative stress for the selective killing of Myc-driven tumors

Matilde Murga^{#1}, Stefano Campaner^{#2}, Andres J. Lopez-Contreras¹, Luis I. Toledo¹, Rebeca Soria¹, Maria F. Montaña¹, Luana D' Artista², Thomas Schleker², Carmen Guerra³, Elena Garcia⁴, Mariano Barbacid³, Manuel Hidalgo⁴, Bruno Amati^{2,5}, and Oscar Fernandez-Capetillo¹

¹Genomic Instability Group, Spanish National Cancer Research Centre (CNIO), Madrid, Spain

²Department of Experimental Oncology, European Institute of Oncology (IEO), at the IFOM-IEO Campus, Milan, Italy

³Experimental Oncology Group, Spanish National Cancer Research Centre (CNIO), Madrid, Spain

⁴Clinical Research Program, Spanish National Cancer Research Centre (CNIO), Madrid, Spain

⁵Center for Genomic Science of IIT@SEMM, Istituto Italiano di Tecnologia (IIT), at the IFOM-IEO Campus, Milan, Italy

These authors contributed equally to this work.

Abstract

Oncogene-induced replicative stress activates an Atr- and Chk1-dependent response, which has been proposed to be widespread in tumors. We here explored whether the presence of replicative stress could be exploited for the selective elimination of cancer cells. To this end, we evaluated the impact of targeting the replicative stress-response on cancer development. In mice, the reduced levels of Atr found on a mouse model of the Atr-Seckel syndrome completely prevented the development of Myc-induced lymphomas or pancreatic tumors, both of which show abundant levels of replicative stress. Moreover, Chk1 inhibitors are very effective in killing Myc-driven lymphomas. In contrast, pancreatic adenocarcinomas initiated by *K-Ras*^{G12V} show no detectable evidence of replicative stress and are non-responsive to this therapy. Besides cancer, Myc overexpression aggravated the phenotypes of Atr-Seckel mice, revealing that oncogenes can modulate the severity of replicative stress-associated diseases.

Correspondence should be addressed to M.M. (mmurga@cno.es) or O.F.-C. (oferandez@cno.es).

Author contributions O.F. designed the study and experiments and wrote the paper. M.M. performed most of the experiments presented. A.J.L. performed the work with the xenografts and the R26-MER^{T2} system. L.I.T. helped with the MycER experiments. L.D., T.S., S.C. and B.A. performed the part on lymphoma chemotherapy and contributed to the discussion of the manuscript. M.F.M. and R.S. helped in the analysis of Seckel MEF, embryos and tumors. C.G. and M.B. helped in the work with *K-Ras*^{G12V}-induced pancreatic tumors. E.G. and M.H. helped in the design and work with the xenograft models.

Introduction

The discovery of intrinsic features that distinguish cancer cells from their normal counterparts carries the promise of being able to selectively target them. In this context, much of the recent efforts in the design of cancer therapies are directed to exploit synthetic lethal interactions with cancer-associated mutations (reviewed in 1). One example of these developments was the finding that poly-ADP-ribose polymerase inhibitors are particularly toxic cells *BRCA* deficient cells^{2,3}; which is currently being explored as a therapeutic strategy for the treatment of breast and ovarian tumors. A complementary approach is to look for synthetic lethal interactions that target a general property, rather than a given mutation, in cancer cells. The presence of certain forms of “stress” might offer such a window.

Cancer cells are characterized by a deregulated cell cycle in which proliferation is not fully coordinated with the rest of cellular activities. This creates imbalances that are the source of stresses such as metabolic or oxidative, to which cancer cells have to adapt by boosting the activity of stress protection pathways⁴. Hence, targeting stress-responsive pathways might be mainly detrimental for cancer cells. Along these lines, a recent report revealed that a small chemical that inhibited the stress response to oxidative stress was selectively toxic for cancer cells⁵. Besides metabolic and oxidative stress, the presence of replicative stress in cancer is now widely recognized⁶. This replicative stress would be originated by the deregulated S phase progression that is driven by oncogenes^{7,8,9,10}, and would also account for a large fraction of the genome rearrangements found in human tumors¹¹. In mammals, the replicative stress response (RSR) is coordinated by *Atr* and *Chk1* kinases^{12,13}, which jointly suppress the accumulation of RS during replication. We here explored whether targeting the RSR can be exploited for the selective elimination of tumors harboring elevated levels of oncogene-induced replicative stress.

Results

Synthetic lethality between *Myc* and *Atr* *in vivo*

B-cell lymphomas arising on $E\mu$ -myc¹⁴ mice are limited by modulators of the DNA damage response (DDR) such as *Tip60*¹⁵ or *Atm*^{16,17}. However, these tumors also present increased levels of *Chk1* phosphorylation¹⁸, reflecting the concomitant activation of an *Atr*-dependent RSR. To determine the impact of *Atr* on *Myc*-driven tumors, $E\mu$ -myc mice were crossed with a hypomorphic *Atr* mouse strain (*Atr*-Seckel; *Atr*^{S/S})¹⁹. As reported, *Atr*^{S/S} mice were born at submendelian ratios¹⁹. However, whereas $E\mu$ -myc⁺ animals were born normally on an *Atr* proficient background, the presence of the *Myc* transgene significantly limited the viability of *Atr*^{S/S} mice (Fig. 1a). This observation revealed the *Myc* overexpression was having an effect on embryonic development in the context of reduced *Atr* levels. Accordingly, $E\mu$ -myc increased the number of apoptotic cells on *Atr* mutant embryos, which was accompanied by a higher incidence of cells presenting a pan-nuclear distribution of γ H2ax (Supplementary Fig. 1). This generalized synthetic lethal interaction between *Myc* and *Atr* during embryogenesis was unexpected given that *Myc* overexpression was thought to be restricted to B cells in the $E\mu$ -myc model. However, we find widespread

overexpression of Myc in transgenic tissues, which could account for the systemic effects of E μ -myc on Atr-Seckel development (Supplementary Fig. 2).

Atr hypomorphism prevents Myc-induced lymphomas

We then explored whether the increased levels of Myc had any effect on born *Atr*^{S/S} mice. The presence of the Myc transgene led to a further 40% reduction in the median lifespan of Atr-Seckel mice (Fig. 1b). Strikingly, even though around half of *Atr*^{S/S}; E μ -myc⁺ animals die at about the same age at which *Atr*^{+/+}; E μ -myc⁺ mice do, we never observed a lymphoma on E μ -myc⁺ mice that were hypomorphic for Atr (n= 0/24). Moreover, the reduction in Atr levels prevented the pretumoral expansion of the white blood cell compartment that occurs on young E μ -myc⁺ mice, suggesting that low levels of Atr prevent even the earliest steps of transformation initiated by Myc (Fig 1c). To further force lymphomagenesis we introduced p53 haploinsufficiency²⁰ into the crosses. In this context, every E μ -myc⁺; *p53*^{+/-} mouse invariably develops a full-blown lymphoma at 5 weeks of age (16/16). In contrast, we never observed a lymphoma on the few *Atr*^{S/S}; E μ -myc⁺; *p53*^{+/-} animals that were born (0/5) (Fig 1d). Altogether, these data demonstrate that low levels of Atr prevent the development of B-cell lymphomas initiated by Myc. However, E μ -myc aggravated the phenotypes of Atr-Seckel mice such as microcephaly, micrognathia, pancytopenia or kyphosis (Fig. 2, and data not shown), explaining the reduced lifespan of *Atr*^{S/S}; E μ -myc⁺ mice.

Atr and Chk1 limit Myc-induced RS and apoptosis

To determine the mechanism of this synthetic lethal interaction between Myc and Atr, we evaluated the impact of targeting the RSR on Myc-induced apoptosis. Addition of 4-OHT in MycER-infected MEF led to an activated DDR21, as indicated by the presence of cells presenting high levels of pan-nuclear γ H2ax (Fig. 3a,b). As previously shown, this staining pattern is reflective of replicative stress since it is restricted to S-phase cells and can also be observed for replication protein A (Rpa)^{22,23,24}. Accordingly, 24 hrs of MycER activation led to an accumulation of cells in G2 and the appearance of Rpa foci (Fig. 3c and Supplementary Fig. 3), both of which would be consistent with an accumulation of replicative stress. At 48 hrs, MycER-induced apoptosis coincided with a concomitant loss of cells in the S and G2 phases of the cell cycle, suggesting that a fraction of Myc-induced cell death could be coming from cells suffering from replicative stress (Fig. 2c). Strikingly, *Atr*^{S/S} MEF presented increased levels of Myc-induced γ H2ax and were highly sensitive to Myc-induced apoptosis (Fig. 3b,c). Likewise, Atr²⁴ or Chk1 inhibitors also sensitized cells to MycER induced apoptosis (Supplementary Fig. 4). Importantly, this synthetic lethal effect was even more pronounced in *p53*-deficient cells, which was again associated with higher levels of Myc-induced γ H2ax (Supplementary Fig. 5). Similar observations were made with MEF from a strain in which MycER was knocked-in at the *ROSA26* locus²⁵ (Supplementary Fig. 6). The data above reveal that cells harboring Myc are particularly sensitive to RSR inhibitors through an apoptotic mechanism that is independent of p53.

Therapeutic effect of Chk1 inhibitors on Myc-induced lymphomas

The mouse data presented above revealed that, *in vivo*, reduced Atr levels prevent the development of Myc-induced lymphomas. However, preventing tumor development does not

imply that such a strategy will work for tumor treatment. We thus tested the effect of inhibiting the RSR in a cohort of mice bearing isogenic tumors by transplanting cells from E μ -myc⁺ lymphomas²⁶. When tumors became palpable, recipient mice were intraperitoneally injected with two independent Chk1 inhibitors and the effect of the drugs was assessed after 16 hr. Consistent with the oncogene-induced DDR model^{6,7,8}, Myc-induced lymphomas presented numerous cells with a pan-nuclear staining of γ H2ax (Fig. 4a). Strikingly, the treatment with Chk1 inhibitors promoted a dramatic increase of γ H2ax and apoptosis throughout the lymphoma, at doses at which little apoptosis was elicited on a healthy spleen (Fig. 4a,b and Supplementary Fig. 7). The same effect of Chk1 inhibitors was also found on p53-deficient E μ -myc⁺ lymphomas (data not shown). In agreement with these data, 9 days of therapy with UCN-01 led to a remarkable regression of Myc-induced lymphomas under every measurable parameter including spleen and lymph node size, and the levels of circulating leukocytes in the bloodstream (Fig. 4c,d). Moreover, the efficacy of this approach is not restricted to mice, since Chk1 inhibitors were also very toxic for human Burkitt-lymphoma lines, the sensitivity being maximal on the lymphomas showing the highest levels of Myc (Supplementary Fig. 8a,b). The acute response of human Burkitt-lymphomas to Chk1 inhibitors was kept in the context of a preclinical model of subcutaneous xenografts (Supplementary Fig. 8c–e). Likewise, knockdown of Chk1 in human primary foreskin (BJ) cells increased their sensitivity towards MycER-induced apoptosis (Supplementary Fig. 8f,g). In summary, targeting the RSR elicits a very robust synthetic lethal interaction in Myc-induced lymphomas, which can be exploited for the pharmacological treatment of these tumors even in the absence of a proficient p53 response.

Targeting the RSR in Myc- and Ras-driven tumors

We finally explored to which extent this therapy was extensible to other tumors. As we recently reported for Atr inhibitors²⁴, the selective toxicity of Chk1 inhibitors was not restricted to Myc and could also be observed with other replicative stress-generating oncogenes such as cyclin E17,²⁷ (Supplementary Fig. 9). In contrast, the introduction of an oncogenic allele of *K-Ras* (*K-Ras*^{G12V}) in its endogenous locus did not yield any detectable increase in replicative stress, and cells harboring this oncogene were not particularly sensitive to Chk1 inhibitors (Supplementary Fig. 9). It is important to note that whereas the overexpression of the *Ras* oncogene with retroviral plasmids does generate Atr-restricted DNA damage²⁸, this *in vitro* model does not fully recapitulate the way by which *Ras* induces tumors. In contrast to Myc, *Ras* does not need to be overexpressed and the mutation of *Ras* in its endogenous locus is sufficient to promote malignant transformation^{29,30}. To validate these observations *in vivo*, we compared the efficacy of Chk1 inhibitors in two independent models of pancreatic cancer driven by Myc³¹ or Ras³² oncogenes. Similarly to Myc-induced lymphomas, pancreatic tumors from Ela-myc transgenic mice presented a high frequency of cells with a pan-nuclear γ H2ax staining (Fig. 5a). In contrast, and as previously shown for *K-Ras*^{G12V} induced lung tumors^{33,34}, pancreatic adenocarcinomas obtained through the introduction of an oncogenic *K-Ras*^{G12V} allele did not show any evidences of an activated DDR (Fig. 5b). Moreover, whereas a treatment with Chk1 inhibitors increased the levels of γ H2ax and apoptosis in Myc-induced pancreatic tumors, it did not have any detectable impact on those induced by *Ras* (Fig. 5a–c). Noteworthy, the induction of γ H2ax and apoptosis by Chk1 inhibitors in the Ela-myc model was restricted to

the Myc-overexpressing tumor and was not detected in the neighboring tissues, providing a good example of the synthetic lethal nature of this approach (Fig. 5d).

In contrast to the lymphomas, the effect of Chk1 inhibitors was not curative in the case of Ela-myc pancreatic adenocarcinomas and animals died regardless of the treatment. One possible explanation is that this is linked to the poor drug delivery to the tumor, which is known to be a major limitation for the treatment of pancreatic cancer³⁵. In order to overcome this constrain, we introduced the Ela-myc transgene on an Atr-Seckel background, so that a limited RSR would be constitutive present in the pancreas. Noteworthy, and in contrast to the lymphoid system, the pancreas of Atr-Seckel mice shows no apparent pathologies. However, and whereas at 16 weeks of age all *Atr*^{+/+}; Ela-myc⁺ mice carry several pancreatic ductal adenocarcinomas (PDA) (25/25); none of the *Atr*^{S/S}; Eμ-myc⁺ mice presented detectable tumors (0/4) (Supplementary Fig. 10). Whereas an effective treatment might still demand adjuvant therapies that facilitate drug delivery, these data reinforce the notion that targeting the RSR might be particularly useful in the context of tumors with high levels of replicative stress.

Discussion

The data presented here are consistent with the oncogene-induced DDR model, in which Atm would be limiting tumorigenesis through the activation of p53. Accordingly, Atm has been shown to mediate the induction of p53-dependent apoptosis in Eμ-myc lymphomas^{16,17}. However, since persistent replicative stress leads to chromosomal breaks³⁶, a break–Atm–p53-dependent and a replicative stress–Atr–p53-independent apoptotic response would coexist in tumors. In fact, Myc-induced lymphomas were shown to present both Atm and Chk1 phosphorylation¹⁵ and MycER expressing MEF also show evidences of Atm and Atr activation (Supplementary Fig. 11a). Our work reveals that targeting Atr or Chk1 can specifically exploit the replicative stress–p53-independent apoptotic branch, and thus become an effective therapy for the treatment of tumors showing high levels of replicative stress (Supplementary Fig. 11b). We should note that this strategy is based on the fact that the presence of replicative stress sensitizes cells to RSR inhibitors, and is therefore not exclusive for Chk1 and Myc. Accordingly, neuroblastomas driven by MYC(N) have also been shown to be sensitive to Chk1 inhibition³⁷, and the same synthetic lethal interaction can also be seen with Atr inhibitors and other replicative stress-inducing oncogenes such as cyclin E138. Whereas it is likely that not all tumors concur with the same levels of replicative stress, this could easily be assessed in tumor biopsies and could therefore be used as a predictable biomarker of the effectiveness of Atr or Chk1 inhibitors.

We are aware that the efficacy of Chk1 inhibitors in the clinic has been modest. However, the same thing might have happened if Imatinib or Olaparib would have been tested as general anticancer strategies regardless of whether the tumors were carrying *ABL39* or *BRCA40* mutations, respectively. The benefit of finding a synthetic lethal interaction is that it allows optimizing the efficacy of a therapy by restricting its use to those tumors that are most likely to respond⁴¹. The use of chemical inhibitors of the response to reactive oxygen species (ROS) to target cancer cells with elevated ROS levels has recently provided an example of these ideas⁵. In this context, we hope that the synthetic lethal interaction

described here can be incorporated into the rationale of clinical trials using Atr or Chk1 inhibitors. We believe that these drugs would be mostly useful for the treatment of human cancers with high levels of replicative stress, even more so by focusing on those cases in which p53 is mutated and classical genotoxic chemotherapy has ceased to work.

In what regards to Myc, our data come to reinforce the emerging role of this oncogene in regulating replication under conditions of stress⁴². On one hand, Myc can promote entry into S-phase by stimulating cyclin E-Cdk2 and E2f1 activity⁴³, or by directly stimulating replication⁴⁴. Consistent with this, we detect higher DNA synthesis rates in OHT-treated MycER MEF (Supplementary Fig. 6b). However, several lines of evidence suggest that the increased S phase entry driven by Myc might be prone to replicative stress^{45,46}. Additionally, Myc can also limit Atr signaling by directly affecting the stability of the checkpoint protein Topbp1⁴⁷. Interestingly, part of the Myc transcriptional response is dedicated to limit replicative stress, either by promoting the biosynthesis of nucleotides⁴⁸ or by limiting the Atm-dependent DDR⁴⁹. Thus, among the different oncogenes Myc might be particularly prone to generate replicative stress. Finally, previous work showed that Myc-induced replicative stress was limited by Wrn, an helicase mutated in the progeroid Werner Syndrome (WS)⁴⁶. The fact that Myc increased genomic instability on WS cells suggested that certain cancer-associated mutations could aggravate the phenotypes of progeroid diseases. Our data on Atr-Seckel; E μ -myc mice provide *in vivo* proof of this concept and demonstrate that oncogenes can contribute to the severity of replicative stress-driven syndromes.

Methods

Mice

Atr-Seckel¹⁹, E μ -myc¹⁴, Ela-myc³¹, p53 deficient²⁰ animals have been described before. The induction of Ras-driven pancreatic tumors by the introduction of a *K-Ras*^{G12V} oncogenic allele on elastase expressing cells has also been described³². For preclinical studies, 106 cells derived from E μ -Myc⁺; *ARF*^{-/-} lymphomas were transplanted into syngeneic C57/Bl6 mice by tail vein injection. Treatments started when tumors became palpable, and some of the tumor-bearing mice were injected with vehicle as a control. UCN-01 or SB-218078 (1 mg ml⁻¹ in DMSO) were diluted fiftyfold in 2% (w/v) Na citrate (pH 3.5) and administered at 5 mg per kg. For pancreatic tumors, the presence of tumors was assessed by CT prior to the treatment. Mice were housed under standard conditions at serum-pathogen free facility of the Spanish National Cancer Centre. Upon signs of morbidity or when required, mice were euthanized in accordance with the Guidelines for Humane Endpoints for Animals Used in Biomedical Research.

Whole body imaging

Whole body imaging was performed on anesthetized animals using the *eXplore Vista* PET-CT (GE Healthcare) and a 7 testla Pharmascan (Bruker). MMWKS software (GE Healthcare) was used for the quantification of skeletal parameters.

Cells and reagents

MEF from E13.5 embryos were obtained by standard methods and grown in Dulbecco's Minimum Essential Media (DMEM, Invitrogen, Grand Island, NY, USA) supplemented with 10% (v/v) FBS (Hyclone, Logan, UT). In all experiments with MEF, low passage (less than 3 passages) MEF were used. BJ-hTERT cells were obtained from ATCC. Leukemic lines were a kind gift of M.A. Piris (Spanish National Cancer Research Center). All cells were grown in 3% oxygen to minimize the exposure to reactive oxygen species. UCN-01 (SIGMA), SB-218078 (Santa Cruz Biotechnology) and 4-OHT (SIGMA) were obtained from commercial sources. The Atr inhibitor (ETP-46464) has been recently described by our group²⁴.

IHC

13.5dpc embryos were fixed in formalin and embedded in paraffin for subsequent processing. Consecutive 2.5 μm sections were treated with citrate for antigenic recovery and processed for immunohistochemistry with γH2ax (Upstate), activated caspase 3 (R&D Systems) and c-Myc (SantaCruz Biotechnology) antibodies. Hematoxiline was used to counterstain. Genotyping was performed from a piece of the tail. Whole embryo IHCs were scanned and digitalized with a MIRAX system (Zeiss) for further analysis.

Transduction in MEFs

pBabe-MycER^{puro}, pBabe-puro and pBabe-puro-cycE1 were retrovirally transduced into early passage MEF following standard procedures. Chk1 targeting lentiviruses were obtained from the TRC collection (SIGMA) and used to infect telomerized BJ cells. Infected cells were selected with 1.5 $\mu\text{g ml}^{-1}$ puromycin for 3 days. After selection, cells were seeded in 6-cm diameter plates for cell-cycle analyses or Greiner μClear 96-well plates for High-Throughput Microscopy mediated quantification of the γH2ax signal.

Supplementary Information

Refer to Web version on PubMed Central for supplementary material.

Acknowledgements

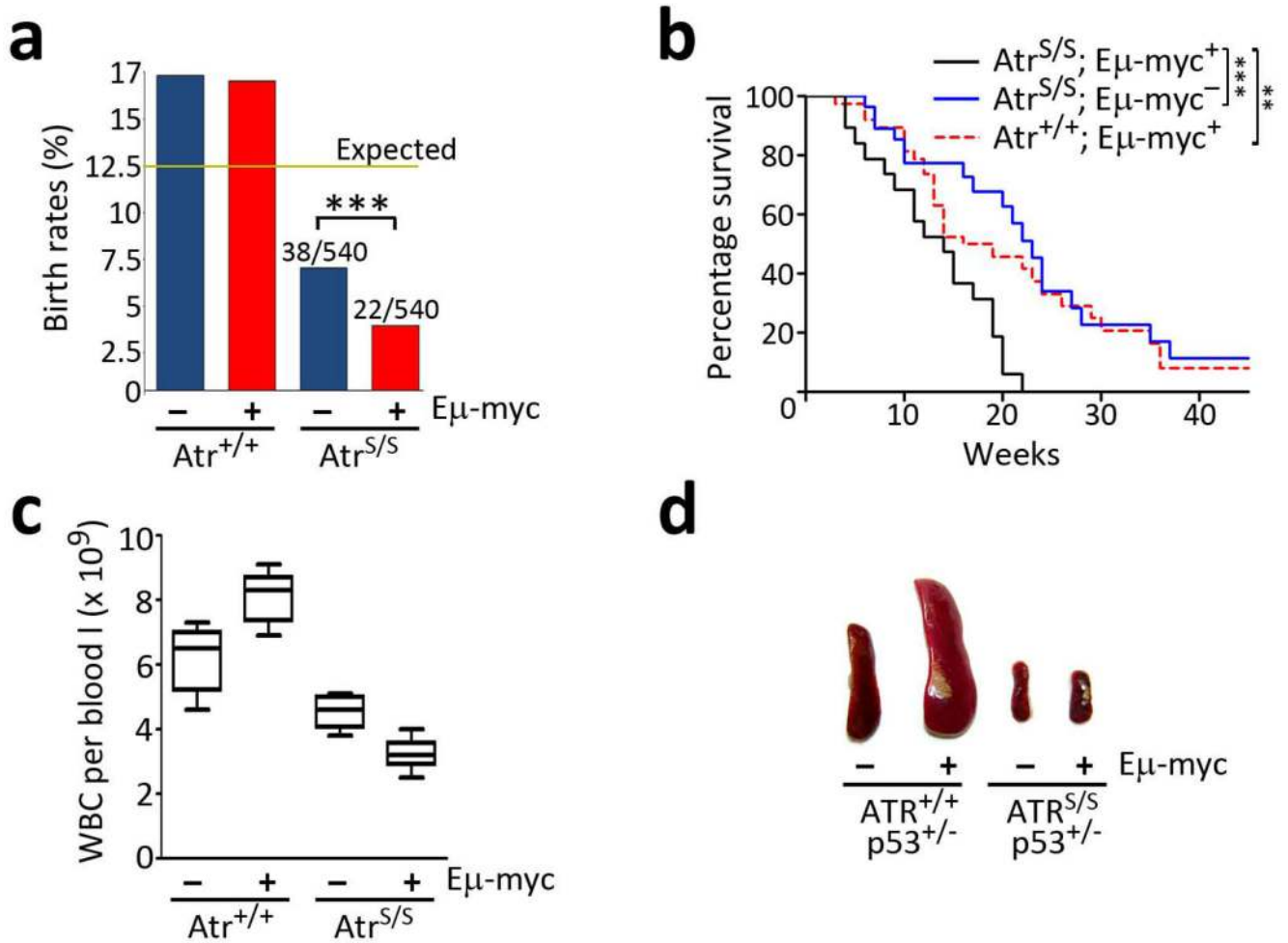
We thank Dr. M. Serrano for critical comments on the manuscript and Dr. F.X. Real for advice on the Ela-myc model. M. M. is supported a grant from Fondo de Investigaciones Sanitarias (PI080220). T. S. is supported by DFG Research Fellowship (SCHL 1945/1-1). Work in O. F.'s laboratory is supported by grants from the Spanish Ministry of Science (CSD2007-00017 and SAF2008-01596), Miguel Catalan Award from the Community of Madrid, EMBO Young Investigator Programme and the European Research Council (ERC-210520).

References

1. de Bono JS, Ashworth A. Translating cancer research into targeted therapeutics. *Nature*. 2010; 467:543–549. [PubMed: 20882008]
2. Bryant HE, et al. Specific killing of BRCA2-deficient tumours with inhibitors of poly(ADP-ribose) polymerase. *Nature*. 2005; 434:913–917. [PubMed: 15829966]
3. Farmer H, et al. Targeting the DNA repair defect in BRCA mutant cells as a therapeutic strategy. *Nature*. 2005; 434:917–921. [PubMed: 15829967]

4. Luo J, Solimini NL, Elledge SJ. Principles of cancer therapy: oncogene and non-oncogene addiction. *Cell*. 2009; 136
5. Raj L, et al. Selective killing of cancer cells by a small molecule targeting the stress response to ROS. *Nature*. 2011; 475:231–234. [PubMed: 21753854]
6. Halazonetis TD, Gorgoulis VG, Bartek J. An oncogene-induced DNA damage model for cancer development. *Science*. 2008; 319:1352–1355. [PubMed: 18323444]
7. Bartkova J, et al. DNA damage response as a candidate anti-cancer barrier in early human tumorigenesis. *Nature*. 2005; 434:864–870. [PubMed: 15829956]
8. Gorgoulis VG, et al. Activation of the DNA damage checkpoint and genomic instability in human precancerous lesions. *Nature*. 2005; 434:907–913. [PubMed: 15829965]
9. Bartkova J, et al. Oncogene-induced senescence is part of the tumorigenesis barrier imposed by DNA damage checkpoints. *Nature*. 2006; 444:633–637. [PubMed: 17136093]
10. Di Micco R, et al. Oncogene-induced senescence is a DNA damage response triggered by DNA hyper-replication. *Nature*. 2006; 444:638–642. [PubMed: 17136094]
11. Dereli-Oz A, Versini G, Halazonetis TD. Studies of genomic copy number changes in human cancers reveal signatures of DNA replication stress. *Mol Oncol*. 2011; 5
12. Cimprich KA, Cortez D. ATR: an essential regulator of genome integrity. *Nat Rev Mol Cell Biol*. 2008; 9:616–627. [PubMed: 18594563]
13. Lopez-Contreras AJ, Fernandez-Capetillo O. The ATR barrier to replication-born DNA damage. *DNA Repair (Amst)*. 2010; 9:1249–1255. [PubMed: 21036674]
14. Harris AW, et al. The E mu-myc transgenic mouse. A model for high-incidence spontaneous lymphoma and leukemia of early B cells. *J Exp Med*. 1988; 167:353–371. [PubMed: 3258007]
15. Gorrini C, et al. Tip60 is a haplo-insufficient tumour suppressor required for an oncogene-induced DNA damage response. *Nature*. 2007; 448:1063–1067. [PubMed: 17728759]
16. Reimann M, et al. The Myc-evoked DNA damage response accounts for treatment resistance in primary lymphomas in vivo. *Blood*. 2007; 110:2996–3004. [PubMed: 17562874]
17. Shreeram S, et al. Regulation of ATM/p53-dependent suppression of myc-induced lymphomas by Wip1 phosphatase. *J Exp Med*. 2006; 203:2793–2799. [PubMed: 17158963]
18. Campaner S, et al. Cdk2 suppresses cellular senescence induced by the c-myc oncogene. *Nat Cell Biol*. 2009; 12:54–59. [PubMed: 20010815]
20. Jacks T, et al. Tumor spectrum analysis in p53-mutant mice. *Curr Biol*. 1994; 4:1–7. [PubMed: 7922305]
21. Vafa O, et al. c-Myc can induce DNA damage, increase reactive oxygen species, and mitigate p53 function: a mechanism for oncogene-induced genetic instability. *Mol Cell*. 2002; 9:1031–1044. [PubMed: 12049739]
22. Gagou ME, Zuazua-Villar P, Meuth M. Enhanced H2AX phosphorylation, DNA replication fork arrest, and cell death in the absence of Chk1. *Mol Biol Cell*. 2010; 21:739–752. [PubMed: 20053681]
23. Syljuasen RG, et al. Inhibition of human Chk1 causes increased initiation of DNA replication, phosphorylation of ATR targets, and DNA breakage. *Mol Cell Biol*. 2005; 25
24. Toledo LI, et al. A cell-based screen identifies ATR inhibitors with synthetic lethal properties for cancer associated mutations. *Nat Struct & Mol Biol*. 2011; 18:721–727. [PubMed: 21552262]
25. Murphy DJ, et al. Distinct thresholds govern Myc's biological output in vivo. *Cancer Cell*. 2008; 14:447–457. [PubMed: 19061836]
26. Schmitt CA, et al. A senescence program controlled by p53 and p16INK4a contributes to the outcome of cancer therapy. *Cell*. 2002; 109
27. Spruck CH, Won KA, Reed SI. Deregulated cyclin E induces chromosome instability. *Nature*. 1999; 401:297–300. [PubMed: 10499591]
28. Gilad O, et al. Combining ATR suppression with oncogenic Ras synergistically increases genomic instability, causing synthetic lethality or tumorigenesis in a dosage-dependent manner. *Cancer Res*. 2010; 70:9693–9702. [PubMed: 21098704]
29. Guerra C, et al. Tumor induction by an endogenous K-ras oncogene is highly dependent on cellular context. *Cancer Cell*. 2003; 4:111–120. [PubMed: 12957286]

30. Jackson EL, et al. Analysis of lung tumor initiation and progression using conditional expression of oncogenic K-ras. *Genes Dev.* 2001; 15:3243–3248. [PubMed: 11751630]
31. Sandgren EP, Quaipe CJ, Paulovich AG, Palmiter RD, Brinster RL. Pancreatic tumor pathogenesis reflects the causative genetic lesion. *Proc Natl Acad Sci U S A.* 1991; 88:93–97. [PubMed: 1986386]
32. Guerra C, et al. Chronic pancreatitis is essential for induction of pancreatic ductal adenocarcinoma by K-Ras oncogenes in adult mice. *Cancer Cell.* 2007; 11:291–302. [PubMed: 17349585]
33. Efeyan A, et al. Limited role of murine ATM in oncogene-induced senescence and p53-dependent tumor suppression. *PLoS One.* 2009; 4:e5475. doi: 10.1371/journal.pone.0005475 [PubMed: 19421407]
34. Junttila MR, et al. Selective activation of p53-mediated tumour suppression in high-grade tumours. *Nature.* 2010; 468:567–571. [PubMed: 21107427]
35. Olive KP, et al. Inhibition of Hedgehog signaling enhances delivery of chemotherapy in a mouse model of pancreatic cancer. *Science.* 2009; 324:1457–1461. [PubMed: 19460966]
36. Hanada K, et al. The structure-specific endonuclease Mus81 contributes to replication restart by generating double-strand DNA breaks. *Nat Struct Mol Biol.* 2007; 14:1096–1104. [PubMed: 17934473]
37. Cole KA, et al. RNAi screen of the protein kinome identifies checkpoint kinase 1 (CHK1) as a therapeutic target in neuroblastoma. *Proc Natl Acad Sci U S A.* 2011; 108:3336–3341. [PubMed: 21289283]
38. Toledo LI, Murga M, Fernandez-Capetillo O. Targeting ATR and Chk1 kinases for cancer treatment: A new model for new (and old) drugs. *Mol Oncol.* 2011; 5:368–373. [PubMed: 21820372]
39. Druker BJ, et al. Effects of a selective inhibitor of the Abl tyrosine kinase on the growth of Bcr-Abl positive cells. *Nat Med.* 1996; 2:561–566. [PubMed: 8616716]
40. Fong PC, et al. Inhibition of poly(ADP-ribose) polymerase in tumors from BRCA mutation carriers. *N Engl J Med.* 2009; 361:123–134. [PubMed: 19553641]
41. Hartwell LH, Szankasi P, Roberts CJ, Murray AW, Friend SH. Integrating genetic approaches into the discovery of anticancer drugs. *Science.* 1997; 278:1064–1068. [PubMed: 9353181]
42. Herold S, Herkert B, Eilers M. Facilitating replication under stress: an oncogenic function of MYC? *Nat Rev Cancer.* 2009; 9:441–444. [PubMed: 19461668]
43. Pickering MT, Stadler BM, Kowalik TF. miR-17 and miR-20a temper an E2F1-induced G1 checkpoint to regulate cell cycle progression. *Oncogene.* 2009; 28
44. Dominguez-Sola D, et al. Non-transcriptional control of DNA replication by c-Myc. *Nature.* 2007; 448:445–451. [PubMed: 17597761]
45. Jacome A, Fernandez-Capetillo O. Lac operator repeats generate a traceable fragile site in mammalian cells. *EMBO Rep.* 2011; 12:1032–1038. [PubMed: 21836640]
46. Robinson K, Asawachaicharn N, Galloway DA, Grandori C. c-Myc accelerates S-phase and requires WRN to avoid replication stress. *PLoS One.* 2009; 4:e5951. doi: 10.1371/journal.pone.0005951 [PubMed: 19554081]
47. Herold S, et al. Miz1 and HectH9 regulate the stability of the checkpoint protein, TopBP1. *EMBO J.* 2008; 27:2851–2861. [PubMed: 18923429]
48. Liu YC, et al. Global regulation of nucleotide biosynthetic genes by c-Myc. *PLoS One.* 2008; 3:e2722. doi: 10.1371/journal.pone.0002722 [PubMed: 18628958]
49. Gordan JD, Bertout JA, Hu CJ, Diehl JA, Simon MC. HIF-2 α promotes hypoxic cell proliferation by enhancing c-myc transcriptional activity. *Cancer Cell.* 2007; 11:335–347. [PubMed: 17418410]

**Fig. 1.**

Reduced levels of Atr prevent lymphomagenesis on Eμ-myc mice. **(a)** Observed birth rates of the different genotypes obtained from Atr^{S/S}; Eμ-myc⁺ x Atr^{+/+}; Eμ-myc⁻ crosses (n = 512 mice; χ^2 : P<0.001). **(b)** Kaplan Meyer analysis of the indicated genotypes (Atr^{S/S}; Eμ-myc⁺: 24; Atr^{+/+}; Eμ-myc⁺: 31; Atr^{S/S}; Eμ-myc⁻: 32). The asterisks indicate the statistical significance of the different survival curves obtained in the Log-Rank Mantel-Cox Test. There was no significant difference between the survival of Atr^{S/S} and Eμ-myc⁺ single mutants (p=0.48). **(c)** White blood cell (WBC) counts from 2 old month mice without detectable lymphoma (n=5). Note the expansion of the WBC compartment on Atr^{+/+}; Eμ-myc⁺ mice, which contrasts with the further depletion of WBC when the Eμ-myc transgene is combined with Atr hypomorphism. **(d)** Photograph of the spleens of 5-week old mice illustrating the absence of splenomegaly on Atr^{S/S}; Eμ-myc⁺; p53^{+/-} mice. (*: P<0.05; **: P<0.01; ***: P<0.001)

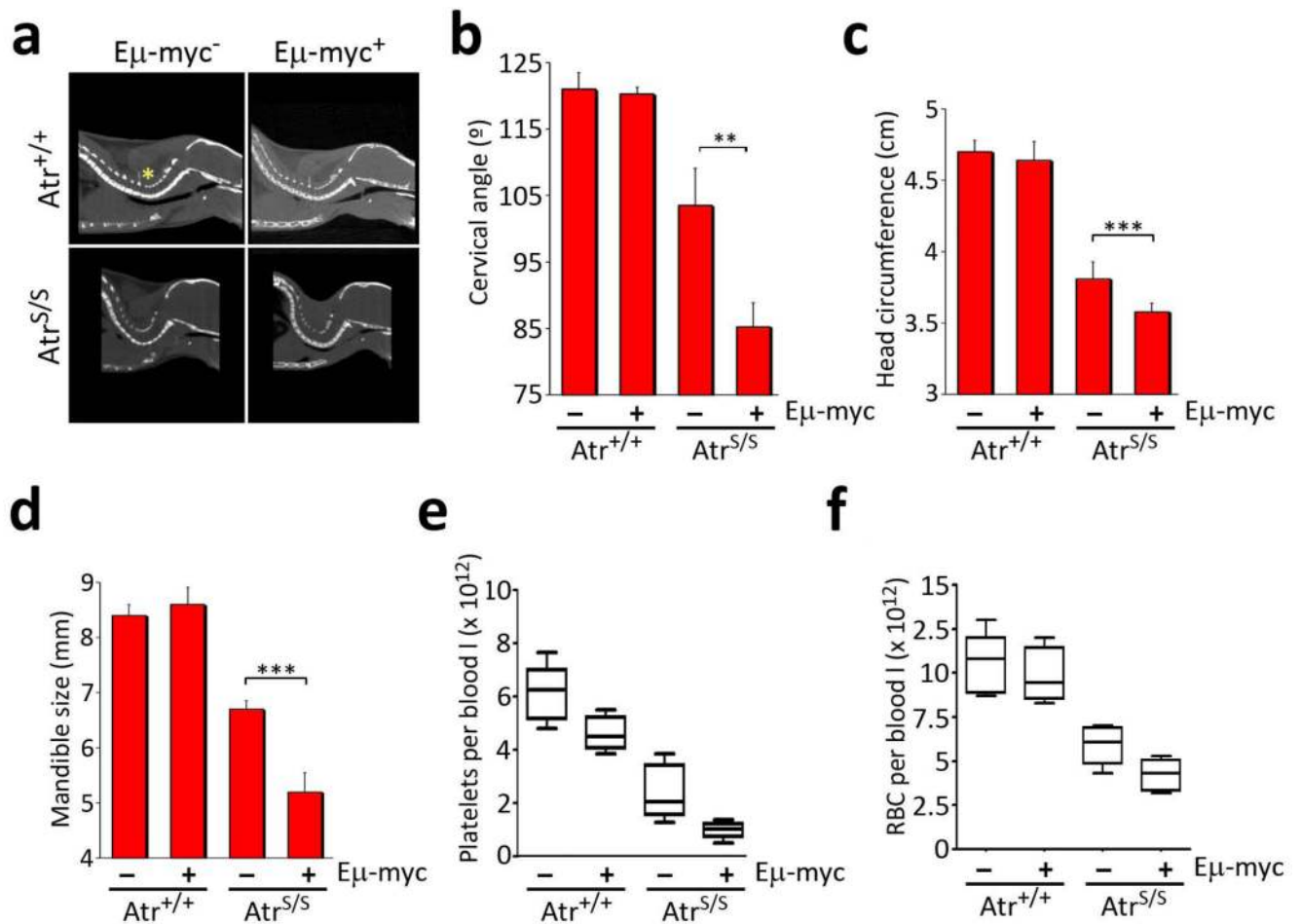


Fig. 2. Eμ-myc aggravates the symptoms of the Seckel Syndrome. **(a)** Representative images of the computerized tomography (CT) analysis of the spine, illustrating the angle used for the cervical angle measurements (yellow asterisk). **(b)** Measurements made from **(a)**. **(c)** Head circumference and **(d)** right mandible size from 2.5 month old mice of the indicated genotypes were calculated from CT analysis of the crania. (n=6; **: $P < 0.01$; ***: $P < 0.001$) **(e)** Platelet and **(f)** red-blood cell (RBC) counts from 2 old month mice without detectable lymphoma (n=5).

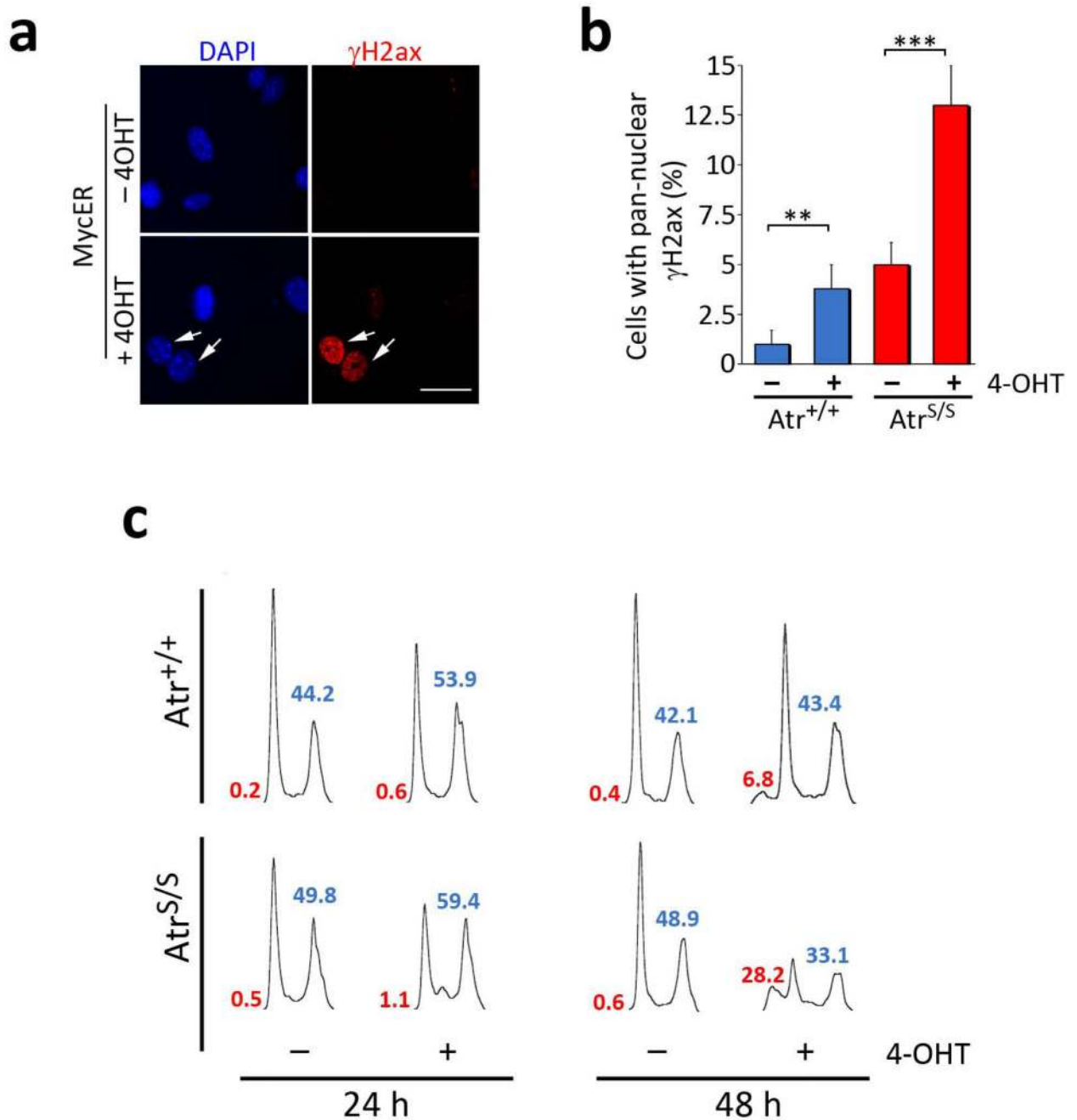


Fig. 3. Atr suppresses Myc-induced RS and apoptosis. (a) Images illustrating the staining pattern of the γ H2ax (red) signal on MycER infected MEF. Scale bar indicates 10 μ m. (b) Percentage of cells showing a pan-nuclear distribution of γ H2ax in MycER infected MEF of the different genotypes in the presence or absence of 4-OHT for 24 hrs. (c) Cell cycle profiles of MycER infected MEF of the different genotypes in the presence or absence of 4-OHT for 24 or 48 hrs. Sub-G1 (red) and S+G2 (blue) percentages are indicated. The images show a

representative experiment that was repeated 3 times with independent MEF pairs. (**:
 $P < 0.01$; ***: $P < 0.001$)

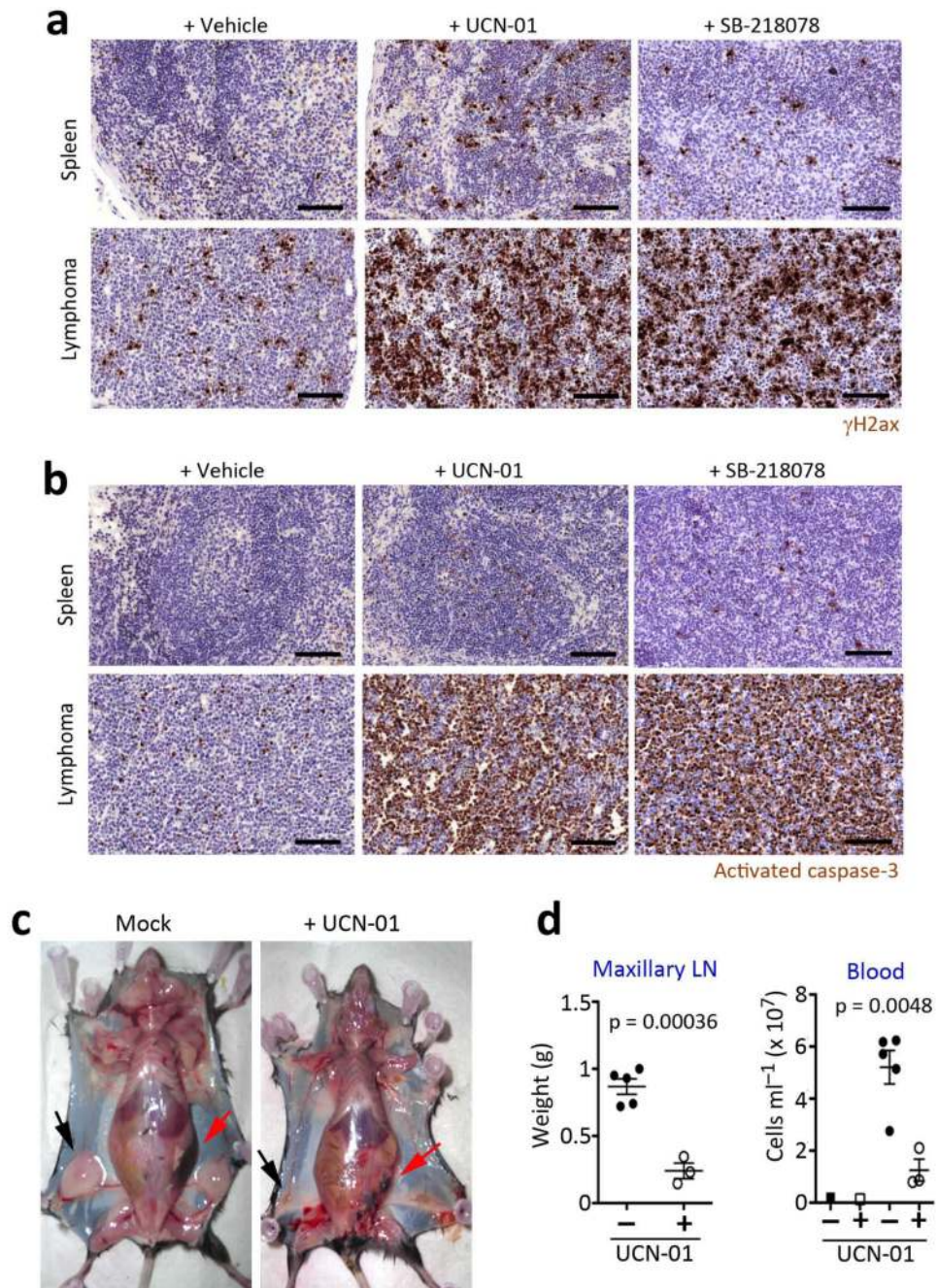


Fig. 4. Treatment of Myc-induced lymphomas with Chk1 inhibitors. Representative images of (a) γ H2ax and (b) activated caspase-3 (C3A) immunohistochemistry (IHC) done on the spleens of mice with or without Myc-induced lymphomas, after a 16 hr treatment with UCN-01 or SB-218078 (5 mg per kg). Black scale bars indicate 100 μm . (c) Representative images of mice carrying Myc-induced lymphomas with or without a daily treatment of UCN-01 (5 mg per kg) for 9 days. The arrows indicate the enlarged lymph nodes (black) and spleen (red) present in the mice carrying Myc-induced lymphomas to illustrate the regression of the

tumor upon treatment. **(d)** Weights of the maxillary lymph nodes and total blood cell counts from the mice mentioned in **(c)**.

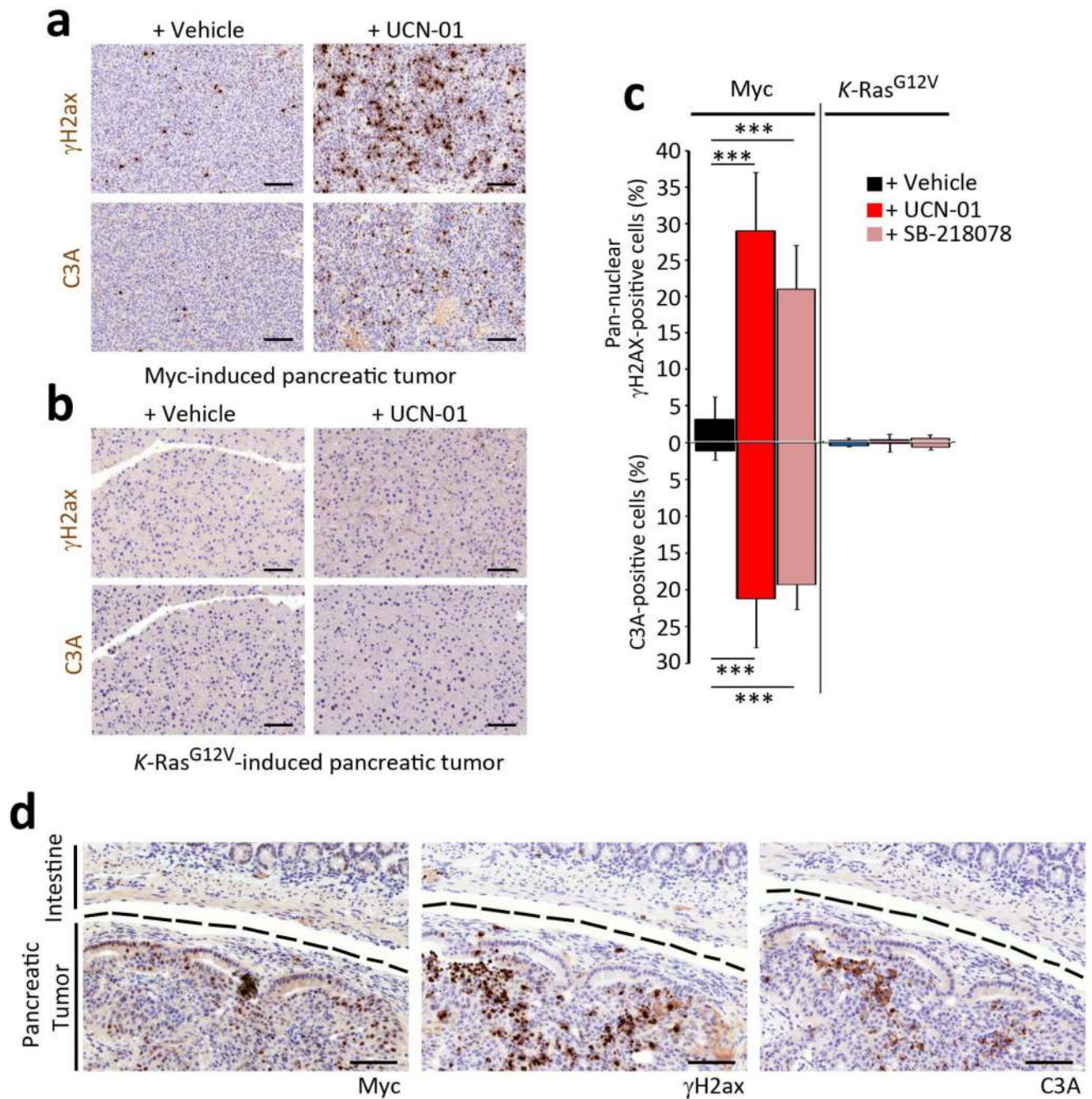


Fig. 5. Effect of Chk1 inhibitors in Myc- or Ras-driven pancreatic tumors. Representative images of γ H2ax and activated caspase-3 (C3A) IHC done on pancreatic tumors obtained from (a) Ela-myc or (b) *K-Ras*^{G12V}-knockin mice, after 3 days of treatment with UCN-01 (i.p. 5 mg per kg). Black scale bars indicate 100 μ m. (c) Quantification from the analysis presented in (a,b). (d) γ H2ax, C3A and c-Myc IHC on the pancreatic tumor from an Ela-myc mouse

after a 3 day treatment with UCN-01 (i.p. 5 mg per kg). A dashed black line separates the tumoral area from the neighbouring intestine. Black scale bars indicate 100 μm .